Available online at www.sciencedirect.com
ScienceDirect
Comput. Methods Appl. Mech. Engrg. 287 (2015) 54–68
Computer methods in applied mechanics and engineering
www.elsevier.com/locate/cma

A new approach for computing hyper-singular interface stresses in IIBEM for solving multi-medium elasticity problems

Kai Yang, Wei-Zhe Feng, Xiao-Wei Gao*

State Key Laboratory of Structural Analysis for Industrial Equipment, Dalian University of Technology, Dalian 116024, China

Received 19 July 2014; received in revised form 4 January 2015; accepted 6 January 2015
Available online 14 January 2015

Abstract

In this paper, a single stress integral equation is presented for solving multi-medium elasticity problems, and by using a newly proposed method for treating arbitrarily high order of singular boundary integrals, a new method is developed for computing the stresses on the interfaces of multi-media. Comparing to conventional multi-domain boundary element methods, the presented Interface Integral BEM (IIBEM) is more efficient in computational time, data preparing, and program coding. However, a big issue is encountered in IIBEM when computing the stresses on interfaces since the commonly used traction-recovery method in computing outer boundary stresses cannot be applied on the interfaces. Therefore, a direct method for handling a hyper-singular stress interface integral equation has to be used to obtain the interface stresses. In the direct method used in the paper, singularities are analytically removed by expressing the non-singular part of the integration kernel as a power series in a local distance defined on a projection line/plane, and the stresses on the interfaces can be evaluated precisely. Numerical examples are given to verify the correctness of the derived boundary-interface integral equations.

Keywords: Multi-medium problems; Boundary-interface integral equation; Boundary element method; Interface stress

1. Introduction

Quite a wide range of engineering problems involves objects composed of different materials. However, there is not yet a boundary integral equation available to solve the multi-medium elastic problems, since the existing boundary integral equations were established for single-medium problems. In order to solve the multi-medium problems using the Boundary Element Method (BEM), the most popular conventional technique is the Multi-Domain Boundary Element Method (MDBEM) [1–6]. The basic idea behind MDBEM is that the whole domain of concern is broken up into separate sub-domains according to the material properties, and a boundary integral equation is written for each sub-domain. The final system of equations is formed by assembling all contributions of discretized boundary integral equations for each sub-domain based on the compatibility condition of displacement and the equilibrium condition of traction at common interface nodes.

* Corresponding author.
E-mail address: xwgao@dlut.edu.cn (X.-W. Gao).

http://dx.doi.org/10.1016/j.cma.2015.01.006
0045-7825/

Although MDBEM is very flexible in solving multi-medium problems, especially large-scale engineering problems, when using an advanced system equation solver [1,4], it takes relatively long computational time since the boundary integrals over interface elements need to be carried out twice. For the same reason, due to the opposing outward normal directions to interfaces which are shared by two adjacent sub-domains, the element information defined over interface needs to be input twice. In addition, the efficiency of MDBEM heavily relies on the assembling technique of the system of equations. This gives rise to some difficulties in coding a universal program.

Recently, a new BEM, the interface integral boundary element Method (IIBEM), was developed by Gao et al. [7,8], which not only can use a single integral equation to solve multi-medium problems, but also can save computational time. However, no stresses on interface nodes were computed in [7,8], since there will be hyper-singular integrals appearing in the resulted integral equations. In this paper, a new single boundary integral equation which is capable of computing interface stresses is developed. Firstly based on a general nonhomogeneous elastic stress–strain relationship, displacement and stress boundary-domain integral equations are established using the Source Point Isolation Method [9]. Then the domain integral included in the nonhomogeneous BEM formulation is degenerated into an interface integral by expressing the variation effect of the shear modulus as the difference of shear moduli between two adjacent materials. The lately proposed hyper-singular integral method [10] is adopted to evaluate the hyper-singular integrals appearing in the stress boundary integral equation. The derived integral equations are very simple in form and only require integration once over the interface elements. Therefore, it is efficient in program coding, input data preparing, and computational time reduction. Numerical examples are provided to demonstrate the potential of the presented formulation.

2. Review of boundary-domain integral equations for single elastic medium with varying modulus

Consider an isotropic, continuously non-homogeneous and linear elastic solid material. In the absence of body forces, the equilibrium equation is given by

$$\sigma_{jk,k} = 0 \tag{1}$$

where σ_{jk} represents the stress tensor, a comma after a quantity represents spatial derivatives and repeated indexes denote summation. It is assumed that the shear modulus μ of the material depends on Cartesian coordinates while Poisson's ratio ν is constant. Under this assumption, the stress tensor σ_{jk} and the displacement gradient $u_{k,l} = \partial u_k/\partial x_l$ are related by the following generalized Hooke's law:

$$\sigma_{ij} = D_{ijkl}u_{k,l} = \mu D^0_{ijkl}u_{k,l} \tag{2}$$

where D^0_{ijkl} is a constant tensor [11]. The weak-form of the equilibrium equation (1) can be written as follows:

$$\int_{\bar{\Omega}} U_{ij}(\boldsymbol{x},\boldsymbol{y})\sigma_{jk,k}(\mathbf{x})d\Omega = 0 \tag{3}$$

where $U_{ij}(\mathbf{x},\boldsymbol{y})$ is a weight function, which is taken as the Kelvin displacement fundamental solution in this paper. Substitution of Eq. (2) into Eq. (3) and application of Gauss's divergence theorem yield [12]

$$c\tilde{u}_i(\boldsymbol{y}) = \int_{\Gamma} U_{ij}(\boldsymbol{x},\boldsymbol{y})t_j(\boldsymbol{x})d\Gamma(\boldsymbol{x}) - \int_{\Gamma} T_{ij}(\boldsymbol{x},\boldsymbol{y})\tilde{u}_j(\boldsymbol{x})d\Gamma(\boldsymbol{x}) + \int_{\bar{\Omega}} V_{ij}(\boldsymbol{x},\boldsymbol{y})\tilde{u}_j(\boldsymbol{x})d\Omega(\boldsymbol{x}) \tag{4}$$

where $c = 1$ for internal points and $c = 0.5$ for smooth boundary nodes. The fundamental solutions U_{ij} and T_{ij} appearing in Eq. (4) can be found in any elasticity BEM book, e.g. [11] and the kernel function V_{ij} can be expressed as follows:

$$V_{ij} = \frac{-1}{4\pi\alpha(1-\nu)r^{\alpha}}\left\{r_{,k}\tilde{\mu}_{,k}[(1-2\nu)\delta_{ij} + \beta r_{,i}r_{,j}] + (1-2\nu)(\tilde{\mu}_{,i}r_{,j} - \tilde{\mu}_{,j}r_{,i})\right\} \tag{5}$$

in which, $\beta = 2$ (2D) or $\beta = 3$ (3D), $\alpha = \beta - 1$, δ_{ij} is the delta symbol and r the distance between the source point y and the field point x.

$\tilde{u}_i(\mathbf{x})$ and $\tilde{\mu}(\mathbf{x})$ are the normalized displacements and shear modulus defined as follows:

$$\tilde{u}_i(\mathbf{x}) = \mu(\mathbf{x})u_i(\mathbf{x}) \tag{6}$$

$$\tilde{\mu}(\mathbf{x}) = \ln \mu(\mathbf{x}). \tag{7}$$

From the expression of Eq. (6), it follows that

$$\frac{\partial u_i}{\partial y_j} = \frac{1}{\mu}\left(\frac{\partial \tilde{u}_i}{\partial y_j} - \tilde{u}_i \frac{\partial \tilde{\mu}}{\partial y_j}\right). \tag{8}$$

Taking the partial derivative of Eq. (4) with respect to the source point $\boldsymbol{y}$, and then substituting the result into Eq. (8) and making use of Eq. (2), we can obtain the following stress integral equation:

$$\sigma_{ij}(\boldsymbol{y}) = \int_\Gamma U_{ijk}(\boldsymbol{x},\boldsymbol{y}) t_k(\boldsymbol{x}) d\Gamma(\boldsymbol{x}) - \int_\Gamma T_{ijk}(\boldsymbol{x},\boldsymbol{y}) \tilde{u}_k(\boldsymbol{x}) d\Gamma(\boldsymbol{x}) + \int_\Omega V_{ijk}(\boldsymbol{x},\boldsymbol{y}) \tilde{u}_k(\boldsymbol{x}) d\Omega(\boldsymbol{x}) + F_{ijk}(\boldsymbol{y}) \tilde{u}_k(\boldsymbol{y}) \tag{9}$$

in which the kernel functions U_{ijk} and T_{ijk} are the same as given in usual BEM books (e.g., [11]), and other quantities are as follows:

$$\begin{aligned} V_{ijk} = {} & \frac{1}{2\pi\alpha(1-\nu)} \frac{1}{r^\beta} \left\{ \beta \tilde{\mu}_{,m} r_{,m} [(1-2\nu)\delta_{ij} r_{,k} + \nu(\delta_{ik} r_{,j} + \delta_{jk} r_{,i}) - \gamma r_{,i} r_{,j} r_{,k}] \right. \\ & \left. + \beta\nu(\tilde{\mu}_{,i} r_{,j} + \tilde{\mu}_{,j} r_{,i}) r_{,k} + (1-2\nu)(\beta \tilde{\mu}_{,k} r_{,i} r_{,j} + \tilde{\mu}_{,j}\delta_{ik} + \tilde{\mu}_{,i}\delta_{jk}) - (1-4\nu)\tilde{\mu}_{,k}\delta_{ij} \right\} \end{aligned} \tag{10}$$

$$F_{ijk} = \begin{cases} \dfrac{-1}{4(1-\nu)} \left((\delta_{ij}\tilde{\mu}_{,k} + \delta_{ik}\tilde{\mu}_{,j} + \delta_{jk}\tilde{\mu}_{,i}) \right) & \text{for 2D} \\ \dfrac{-1}{15(1-\nu)} \left((2+10\nu)\delta_{ij}\tilde{\mu}_{,k} + (7-5\nu)(\delta_{ik}\tilde{\mu}_{,j} + \delta_{jk}\tilde{\mu}_{,i}) \right) & \text{for 3D.} \end{cases} \tag{11}$$

Eqs. (4) and (9) are the basic boundary-domain integral equations for solving a single medium elasticity problem with varying shear modulus. Since the kernel function V_{ij} and V_{ijk} include the spatial derivatives of the shear modulus μ, it is required that the shear modulus should vary continuously within the domain $\bar{\Omega}$. For a problem consisting of multiple materials, the shear modulus jumps across interfaces of different materials. Therefore, Eqs. (4) and (9) cannot be directly used. In the next section, we extend Eqs. (4) and (9) to solve multi-material problems by turning the jump effect of the shear modulus into an interface integral through a degenerate technique.

3. General boundary-domain integral equations for multi-medium elastic problems with varying shear moduli

For the sake of convenience and not losing generality, a problem consisting of two media characterized by shear and strain tensor μ_1 and μ_2 is considered as shown in Fig. 1. Γ is the outer boundary of the problem, Γ_I represents the interface between media Ω_1 and Ω_2, and n' is the outer unit normal to Ω_1. Since the shear and strain tensor jumps across the interface Γ_I, we separate a narrow domain Ω_3 around Γ_I, which has a constant infinitesimal thickness Δh along the interface.

Referring to Fig. 1 and Ref. [8], the domain integral in Eq. (4) can be written as

$$\int_{\bar{\Omega}} V_{ij}\tilde{u}_j d\Omega = \int_\Omega V_{ij}\tilde{u}_j d\Omega + \lim_{\Delta h \to 0} \left(\Delta h \int_{\Gamma_I} V_{ij}\tilde{u}_j d\Gamma \right) \tag{12}$$

where Ω represents the whole domain consisting of all media and V_{ij} is determined by Eq. (5). To evaluate gradients of the normalized shear modulus $\tilde{\mu}$ involved in the kernel V_{ij}, substituting Eq. (5) into Eq. (12) and noticed that after taking the limit process, i.e. letting $\Delta h \to 0$, the first term on the right-hand side of Eq. (12) is zero, thus, referring to Ref. [8], it follows that

$$\int_{\bar{\Omega}} V_{ij}\,\tilde{u}_j d\Omega = \int_\Omega V_{ij}\,\tilde{u}_j d\Omega + \int_{\Gamma_I} T'_{ij}\,\Delta\mu u_j d\Gamma \tag{13}$$

where

$$T'_{ij} = \Sigma_{ijl} n'_l = \frac{-1}{4\pi\alpha(1-\nu)r^\alpha} \left\{ r_{,k} n'_k [(1-2\nu)\delta_{ij} + \beta r_{,i} r_{,j}] + (1-2\nu)(n'_i r_{,j} - n'_j r_{,i}) \right\}. \tag{14}$$

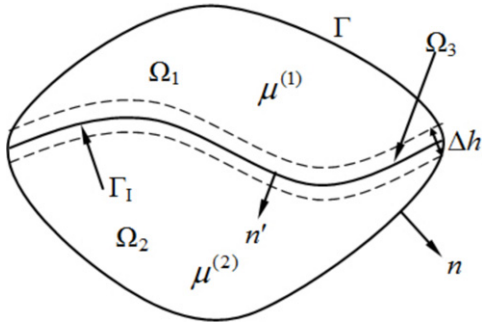

Fig. 1. A narrow domain separated around interface of two media.

Finally, substituting Eq. (13) into Eq. (4), it follows that

$$c\tilde{u}_i(\mathbf{y}) = \int_\Gamma U_{ij}(\mathbf{x},\mathbf{y})t_j(\mathbf{x})d\Gamma - \int_\Gamma T_{ij}(\mathbf{x},\mathbf{y})\tilde{u}_j(\mathbf{x})d\Gamma + \int_{\Gamma_I} \Delta\mu T'_{ij}u_j(\mathbf{x})d\Gamma(\boldsymbol{x}) + \int_\Omega V_{ij}(\boldsymbol{x},\mathbf{y})\tilde{u}_j(\boldsymbol{x})d\Omega(\boldsymbol{x}). \tag{15}$$

In the numerical implementation of Eq. (15), three types of points are defined in discretization: outer boundary points on Γ, interface points on Γ_I, and internal points in Ω. Eq. (15) is only suitable for the outer boundary and internal points by setting $c = 0.5$ and $c = 1$ for smooth boundary and internal points, respectively. When the source point $\boldsymbol{y}$ is located on interface points, referring to Ref. [8] it follows that:

$$c = \frac{1}{2}(\mu_1 + \mu_2). \tag{16}$$

Similarly, taking the partial derivative of Eq. (15) with respect to the source point $\boldsymbol{y}$, and then substituting the result into Eq. (8) and making use of Eq. (2), we can obtain the following stress integral equation.

$$\sigma_{ij}(\mathbf{y}) = \int_\Gamma U_{ijk}(\mathbf{x},\mathbf{y})t_k(\mathbf{x})d\Gamma(\mathbf{x}) - \int_\Gamma T_{ijk}(\mathbf{x},\mathbf{y})\tilde{u}_k(\mathbf{x})d\Gamma(\mathbf{x}) + \int_{\Gamma_I} \Delta T'_{ijk}u_j(\mathbf{x})d\Gamma(\mathbf{x}) + \int_\Omega V_{ijk}(\mathbf{x},\mathbf{y})\tilde{u}_k(\mathbf{x})d\Omega(\mathbf{x}) + F_{ijk}(\mathbf{y})\tilde{u}_k(\mathbf{y}) \tag{17}$$

in which the kernel functions U_{ijk} and T_{ijk} are the same as given in Eq. (9), and $\Delta T'_{ijk}$ is evaluated below:

$$\Delta T'_{ijk} = -\Delta D_{ijmn}\Sigma_{mkl,n}n'_l. \tag{18}$$

Eq. (17) can also be applied to interface points.

Comparing Eqs. (15) and (17) for multi-medium varying coefficient elastic problems to those for single-medium ones, Eqs. (4) and (9), it can be seen that the interface integrals are additional terms in the multi-medium problems. These additional terms reflect the effect of shear modulus jump across the interface.

4. Boundary-interface integral equations for piecewise homogeneous problems

Eqs. (15) and (17) are the boundary-interface-domain integral equations for general multi-media varying shear modulus problems. For usual piecewise homogeneous problems, they can be reduced to a simple unified boundary-interface integral equation.

4.1. Boundary-interface integral equation for piecewise homogeneous problems

In piecewise homogeneous problems, the shear modulus μ may be different for different media, but it is constant within each medium. In this case, the domain integrals included in Eqs. (15) and (17) have zero values due to the fact

that the spatial derivatives of the shear modulus μ involved in the kernel V_{ij}, V_{ijk} and F_{ijk} are zero (see Eqs. (5), (10) and (11)). Thus, taking into account relationship (8), Eq. (15) can be reduced to the following unified form:

$$\hat{\mu}u_i(\mathbf{y}) = \int_\Gamma U_{ij}(\mathbf{x},\mathbf{y})t_j(\mathbf{x})d\Gamma(\mathbf{x}) - \int_\Gamma \mu T_{ij}(\mathbf{x},\mathbf{y})u_j(\mathbf{x})d\Gamma(\mathbf{x}) + \int_{\Gamma_I} \Delta\mu T'_{ij}(\mathbf{x},\mathbf{y})u_j(\mathbf{x})d\Gamma(\mathbf{x}) \tag{19}$$

where T'_{ij} is evaluated by Eq. (14), and $\hat{\mu}$ can be written as follows:

$$\hat{\mu} = \begin{cases} \dfrac{1}{2}\mu & \text{for smooth outer boundary points on } \Gamma \\ \dfrac{1}{2}(\mu_1+\mu_2) & \text{for smooth interface points on } \Gamma_I \\ \mu & \text{for internal points.} \end{cases} \tag{20}$$

Similarly, in piecewise homogeneous problems, Eq. (17) can be written as follows:

$$\sigma_{ij}(\mathbf{y}) = \int_\Gamma U_{ijk}(\mathbf{x},\mathbf{y})t_k(\mathbf{x})\mathrm{d}\Gamma_{\mathbf{x}} - \int_\Gamma T_{ijk}(\mathbf{x},\mathbf{y})\tilde{u}_k(\mathbf{x})\mathrm{d}\Gamma_{\mathbf{x}} + \int_{\Gamma_I} \Delta T'_{ijk}(\mathbf{x},\mathbf{y})u_k(\mathbf{x})d\Gamma_{\mathbf{x}} \tag{21}$$

where, in which the kernel functions U_{ijk} and T_{ijk} are the same as given in Eq. (9), for piecewise homogeneous materials $\Delta T'_{ijk}$ is evaluated below:

$$\Delta T'_{ijk}(\mathbf{x},\mathbf{y}) = \frac{\bar{T}_{ijk}(\mathbf{x},\mathbf{y})}{r^\beta}. \tag{22}$$

For 2D problems:

$$\begin{aligned}\bar{T}_{ijk} = {} & \frac{\Delta\mu}{2\pi(1-\upsilon)}\{2r_{,m}n_m[(1-2\upsilon)\delta_{ij}r_{,k} + \upsilon(\delta_{ik}r_{,j} + \delta_{jk}r_{,i}) - 4r_{,i}r_{,j}r_{,k}] \\ & + 2\upsilon(n_i r_{,j}r_{,k} + n_j r_{,i}r_{,k}) + (1-2\upsilon)(2n_k r_{,i}r_{,j} + n_j\delta_{ik} + n_i\delta_{jk}) - (1-4\upsilon)n_k\delta_{ij}\}.\end{aligned} \tag{23}$$

For 3D problems:

$$\begin{aligned}\bar{T}_{ijk} = {} & \frac{\Delta\mu}{4\pi(1-\upsilon)}\{3r_{,m}n_m[(1-2\upsilon)\delta_{ij}r_{,k} + \upsilon(\delta_{ik}r_{,j} + \delta_{jk}r_{,i}) - 5r_{,i}r_{,j}r_{,k}] \\ & + 3\upsilon(n_i r_{,j}r_{,k} + n_j r_{,i}r_{,k}) + (1-2\upsilon)(3n_k r_{,i}r_{,j} + n_j\delta_{ik} + n_i\delta_{jk}) - (1-4\upsilon)n_k\delta_{ij}\}.\end{aligned} \tag{24}$$

From Eq. (14) we can see that the kernel functions T_{ij} and T'_{ij} are strongly singular [13–17] when the source point is located on the outer boundary or the interface element under integration. To avoid direct evaluation of integrals related to these two kernel functions, the "rigid body motion" technique [8,11] is used to determine the coefficient matrices formed by the strongly singular integrals.

When we try to evaluate stresses, there are three cases for different source point locations. When the source point is located in the internal field, Eq. (17) can be directly used to evaluate stresses, since none singularities arise for this case; when the source point is located on the outer boundary, the traction-recovery method [11] can be employed to compute stresses on the outer boundary. However, when the source point is located on the interface, handicap arises, because no tractions exist on the interface and therefore the traction-recovery method cannot be employed. To solve this problem, the stress integral equation has to be used. But when source point is on the interface, the interface integral is hyper-singular with the singular order of β. This indicates that the evaluation of a hyper-singular integral is the key technique to compute interface stresses in IIBEM.

4.2. Evaluation of hyper-singular interface integrals using the newly proposed projection plane method

In order to numerically evaluate the boundary integrals or interfacial integrals shown in Eqs. (19) and (21), coordinates in an element can be expressed in terms of their nodal values as follows:

$$x_i(\xi) = \sum_{\alpha=1}^{N_{node}} N_\alpha(\xi)x_i^\alpha \tag{25}$$

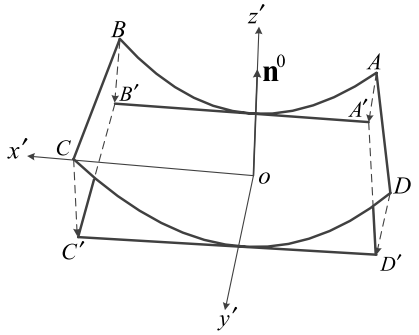

Fig. 2. Boundary element projected onto the projection plane.

where N_{node} is the number of element nodes; ξ represents the intrinsic coordinate (for a surface element it being understood that $(\xi) = (\xi_1, \xi_2)$); N_α is the shape function of the αth node [11], and x_i^α is the ith component of coordinates at the αth node.

From Eq. (22) we can see that the kernel functions $\Delta T'_{ijk}$ is hyper strongly singular when the source point is located on the interface element under integration. Therefore, a particular hyper-singular integral technique is needed to evaluate the following integral:

$$\int_{\Gamma_s} \Delta T'_{ijk}(\mathbf{x}, \mathbf{y}) N_\alpha(x) d\Gamma_{\mathbf{x}} \tag{26}$$

where, $N_\alpha(x)$ is the shape function [11], and Γ_s is the singular interface element containing the source point. If the source point is placed inside an element, then Γ_s consists of just one element; if the source point is on the boundary of an element, Γ_s consists of all adjacent elements shared the source point.

In 3D problems, the boundary element is a curved surface as marked with ABCD in Fig. 2, so direct evaluating integrals over them is difficult. To solve this problem, we introduce a projection plane, which is the tangential plane of the element to the origin of the intrinsic coordinate system. A local orthogonal coordinate system (x', y', z'), or written as (x'_1, x'_2, x'_3), is established on the projection plane with its origin being at the point $(\xi_1 = 0,\ \xi_2 = 0)$, in which axes x'_1 and x'_2 are located within the plane. The axis x'_1 is along ξ_1 direction and axis x'_3 is along the outward normal direction to the element. Assuming that the direction cosine of the local coordinate axes with respective to the global one is L_{ij}, (its determination method can be found in references, i.e., in [10]), the coordinates transformation between the local and global systems can be performed using the following relationships:

$$x'_i = L_{ij}(x_j - x_j^o) \tag{27}$$

$$x_i = x_i^o + L_{ji} x'_j \tag{28}$$

where the repeated subscripts represent summation, x_i^o is the global coordinates of the origin of the local coordinate system, which is determined using Eq. (25) by setting $\xi = 0$.

Making use of Eq. (27), one can project the original curved element onto the projection plane to form a flat projection element, and then all geometry quantities can be expressed in terms of variables defined on the projection plane.

In a plane, there are only two independent variables. We choose x'_1 and x'_2 as the independent variables, and z' (i.e., x'_3) over the curved surface can be expressed in terms of x'_1 and x'_2. To do so, expanding z' as Taylor series about the origin of the local coordinate system as follows (truncated to quadratic terms):

$$z' = a_I(z') x'_I + a_{IJ}(z') x'_I x'_J \tag{29}$$

in which, capital subscripts I and J take values from 1 to 2, and

$$a_I(z') = \frac{\partial z'}{\partial x'_I} = \frac{\partial z'}{\partial \xi_K} \frac{\partial \xi_K}{\partial x'_I} \tag{30}$$

$$a_{IJ}(z') = \frac{1}{2} \left\{ \frac{\partial^2 z'}{\partial \xi_K \partial \xi_L} \frac{\partial \xi_K}{\partial x'_I} \frac{\partial \xi_L}{\partial x'_J} + \frac{\partial z'}{\partial \xi_K} \frac{\partial^2 \xi_K}{\partial x'_I \partial x'_J} \right\} \tag{31}$$

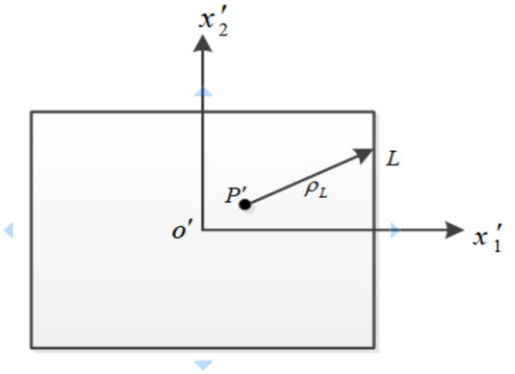

Fig. 3. Quantities defined on the projection plane.

where $\partial z'/\partial \xi_K$ can be calculated by nodal local coordinates using Eq. (25), expressions for $\partial \xi_K/\partial x'_I$ have been given by Lachat in [18], and expressions for $\frac{\partial^2 \xi_k}{\partial x'_I \partial x'_J}$ can be found in [10].

The local distance ρ projected from the global distance r onto the projection plane and its derivatives $\rho_{,I}$ are introduced (see Fig. 3) as follows:

$$\rho = \sqrt{\left(x'_1 - y'_1\right)^2 + \left(x'_2 - y'_2\right)^2} \tag{32}$$

$$\rho_{,I} = \frac{x'_I - y'_I}{\rho}. \tag{33}$$

The local coordinates at the field point can be expressed in terms of a linear relationship on ρ as follows

$$x'_I = y'_I + \rho_{,I}\rho. \tag{34}$$

From Eq. (34) and Fig. 3, it can be seen that $\rho_{,I}$ is a quantity depending on the angle between ρ and axis x'_1, being independent of ρ itself.

Substituting Eq. (34) into Eq. (29) yields:

$$z' = p(z') + q(z', \rho)\rho \tag{35}$$

where,

$$p(z') = a_I(z')y'_I + a_{IJ}(z')y'_I y'_J = z'^p \tag{36}$$

$$q(z', \rho) = q_1(z') + q_2(z')\rho \tag{37}$$

and,

$$q_1(z') = [a_I(z') + 2a_{IJ}(z')y'_J]\rho_{,I} \tag{38a}$$

$$q_2(z') = a_{IJ}(z')\rho_{,I}\rho_{,J}. \tag{38b}$$

In a similar manner to 2D case, intrinsic coordinates can be expressed as:

$$\xi_K = p(\xi_K) + q(\xi_K, \rho)\rho \tag{39}$$

where $p(\xi_K)$ and $q(\xi_K, \rho)$ can be determined by replacing z' with ξ_K in Eqs. (36) and (37).

Substituting Eqs. (34) and (35) into Eq. (28) yields

$$x_i = x_i^p + L_{Ji}\rho_{,J}\rho + L_{3i}q(z', \rho)\rho \tag{40}$$

and then substituting Eq. (37) into above equation results in

$$x_i = y_i + (b_i + c_i\rho)\rho \tag{41}$$

where

$$b_i = L_{Ji}\rho_{,J} + L_{3i}q_1(z') \tag{42a}$$

$$c_i = L_{3i}q_2(z'). \tag{42b}$$

Making use of the normalized orthogonal property of the coordinate transformation tensor L_{ij}, the expansion of r can be derived using Eq. (41) as follows:

$$r = \sqrt{(x_i - y_i)(x_i - y_i)} = g(\rho)\rho \tag{43}$$

where,

$$g(\rho) = \sqrt{1 + q^2(z', \rho)} = \sqrt{G_0 + G_1\rho + G_2\rho^2} \tag{44}$$

here, $G_0 = b_i b_i$, $G_1 = 2b_i c_i$ and $G_2 = c_i c_i$.

It is easy to derive that

$$r_{,i} = \frac{\partial r}{\partial x_i} = \frac{b_i + c_i\rho}{g(\rho)}. \tag{45}$$

After expanding all geometry quantities over an element in terms of the local distance, we can handle the singular boundary integrals shown in Eq. (26).

In 3D problems, the relationship between the differential areas over the projection plane and the real surface can be written as:

$$dA = d\Gamma\cos\phi = d\Gamma n_i^0 n_i \tag{46}$$

in which, A is the area of the projection plane, n_i^0 and n_i are the outward normals to the tangential planes to the origin of the local coordinate system and the field point, and ϕ is the angle between them.

Substituting Eqs. (43) and (46) into Eq. (26), the surface integral can be expressed in terms of an integral over the projection plane as follows:

$$I(\mathbf{y}) = \int_A \frac{\bar{T}_{ijk}(\mathbf{x}, \mathbf{y})}{g^\beta(\rho)\rho^\beta n_i^0 n_i} dA(\mathbf{x}). \tag{47}$$

Employing the Radial Integration Method (RIM) [19–25], the above integral over the projection plane can be transformed into a closed line integral over the contour of the projection element (see Fig. 3):

$$I(\mathbf{y}) = \int_L \frac{1}{\rho}\frac{\partial\rho}{\partial n^L} F dL \tag{48}$$

in which, $\partial\rho/\partial n^L = \rho_{,I} n_I^L$ with n_I^L being the outward normal to the contour line L (Fig. 3), and F is a radial integral on the projection plane and can be written as:

$$F = \lim_{\rho_\varepsilon \to 0} \int_{\rho_\varepsilon}^{\rho_L} \frac{\bar{F}(\rho)}{\rho^{\beta-1}} d\rho \tag{49}$$

where ρ_L is the distance from the source point to the integration point on the contour line L, and $\bar{F}(\rho)$ is the regular part of the integrand in Eq. (47):

$$\bar{F}(\rho) = \frac{\bar{T}_{ijk}(\mathbf{x}(\rho), \mathbf{y})}{g^\beta(\rho) n_i^0 n_i}. \tag{50}$$

In order to integrate Eq. (49), the non-singular part $\bar{F}$ is expanded as a power series in ρ, such that

$$\bar{F}(\rho) = \sum_{n=0}^{N} B^{(n)}\rho^n \tag{51}$$

in which, N is the order of the power series, usually taking a value between 2 and 7 depending the size of ρ_E; and $B^{(n)}$ are constants which are determined by collocating $N+1$ points over the integration region $(0, \rho_E)$. In this paper, $N+1$ equally spaced points are used, i.e., $(0, \rho_1, \ldots, \rho_N)$. The coefficient for the first point $(n=0)$ is $B^{(0)} = \bar{F}(0)$ and other coefficients can be solved using the following equation set:

$$[R]\{B\} = \{Y\} \tag{52}$$

where, $[R]$ is a square matrix with the order of N:

$$[R] = \begin{bmatrix} 1, & \rho_1, & \cdots & \rho_1^{N-1} \\ 1, & \rho_2, & \cdots & \rho_2^{N-1} \\ \vdots & \vdots & \cdots & \vdots \\ 1, & \rho_N, & \cdots & \rho_N^{N-1} \end{bmatrix}. \tag{53}$$

$\{B\}$ and $\{Y\}$ are vectors as follows:

$$\{B\} = \begin{Bmatrix} B^1 \\ B^2 \\ \vdots \\ B^N \end{Bmatrix} \qquad \{Y\} = \begin{Bmatrix} [\bar{F}(\rho_1) - B^{(0)}]/\rho_1 \\ [\bar{F}(\rho_2) - B^{(0)}]/\rho_2 \\ \vdots \\ [\bar{F}(\rho_N) - B^{(0)}]/\rho_N \end{Bmatrix}. \tag{54}$$

Solving Eq. (52) for coefficient vector $\{B\}$ and then substituting Eq. (51) into (50) yield:

$$F = \sum_{n=0}^{N} B^{(n)} \lim_{\varepsilon \to 0} \int_{\varepsilon}^{\rho_E} \rho^{n-\beta} d\rho = \sum_{n=0}^{N} B^{(n)} E_n \tag{55}$$

where,

$$E_n = \begin{cases} \dfrac{1}{n-\beta+1} \left(\dfrac{1}{{\rho_E}^{\beta-n-1}} - \lim\limits_{\rho_\varepsilon \to 0} \dfrac{1}{{\rho_\varepsilon}^{\beta-n-1}} \right) & (n \neq \beta - 1) \\ \ln \rho_E - \lim\limits_{\rho_\varepsilon \to 0} \ln \rho_\varepsilon & (n = \beta - 1). \end{cases} \tag{56}$$

For a physical problem, the integral should exist. This means that the infinite terms involved in above equation should be eliminated after considering the contributions of all adjacent elements around the source point or should be canceled out by free terms [10,11]. Thus, after a tedious derivation [10], Eq. (56) becomes

$$E_n = \begin{cases} \dfrac{1}{n-\beta+1} \left(\dfrac{1}{{\rho_E}^{\beta-n-1}} - H_{\beta-n-1} \right) & (0 \leq n \leq \beta - 2) \\ \ln \rho_E - \ln H_0 & (n = \beta - 1) \\ \dfrac{1}{n-\beta+1} {\rho_E}^{n-\beta+1} & (n > \beta - 1) \end{cases} \tag{57}$$

where

$$H_0 = \frac{1}{\sqrt{G_0}}, \qquad H_1 = \frac{G_1}{2G_0}, \qquad H_2 = \frac{G_2}{G_0} - \frac{{G_1}^2}{2{G_0}^2} \tag{58a}$$

$$H_3 = \frac{3G_3}{2G_0} - \frac{3G_1G_2}{2{G_0}^2} + \frac{{G_1}^3}{2{G_0}^3} \tag{58b}$$

$$H_4 = \frac{2G_4}{G_0} - \frac{2G_1G_3 + {G_2}^2}{{G_0}^2} + \frac{2{G_1}^2G_2}{{G_0}^3} - \frac{{G_1}^4}{2{G_0}^4}. \tag{58c}$$

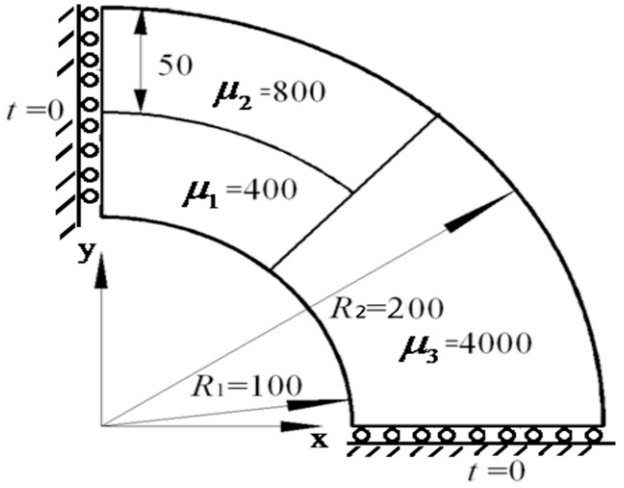

Fig. 4. A quarter of thick-wall cylinder consisting of three media.

Here,

$$G_0 = b_i b_i, \qquad G_1 = 2b_i c_i, \qquad G_2 = c_i c_i \tag{59}$$

in which, b_i and c_i are determined by Eq. (42).

Since ρ_L is the distance from the projected source point P' to the contour line L (see Fig. 3), ρ_L is not zero when P' is located at interior of the element. Otherwise, when P' is located on a side of L, the value of $\partial\rho/\partial n^L$ on the current element has the same size but opposite sign to that on the adjacent element, and therefore they are canceled out each other. This means that the sides where P' is located on need not to be considered at all. Thus, arbitrary order of singular surface integrals can be evaluated using Eqs. (48), (55) and (57) without any singularities.

5. Numerical examples

Based on the code in [8], a computer code has been developed using the formulations derived in this paper. This code can use linear and quadratic boundary elements. Two examples with piecewise homogeneous materials are presented in the following and computational results are compared with those from the Finite Element Method (FEM) and MDBEM [4] to verify the correctness of the developed formulations.

Example 1 (*Thick-Walled Cylinder Consisting of Three Media Under Internal Pressure*)**.** A thick cylinder, consisting of three media, with an internal diameter of 200 units and an external diameter of 400 units, is subjected to an internal pressure of ten units ($P = 10$) under the plane strain condition.

Due to symmetry, a quarter of the cylinder is analyzed. The geometry and boundary conditions of this example are shown in Fig. 4. The material properties are: shear modules of elasticity $\mu_1 = 400$, $\mu_2 = 800$, $\mu_3 = 4000$, and Poisson's ratio $\nu = 0.25$. Both the inner and outer circumferential lines are discretized into 12 equally-spaced quadratic boundary elements; the middle curved line, the interface, is discretized into 6 continuous equally-spaced quadratic boundary elements, respectively; and each of the three straight lines along the radial direction is discretized into 10 equally-spaced quadratic elements. The whole BEM model has a total of 44 outer boundary elements and 16 interface elements and 138 nodes, of which there are 8 inner nodes. Fig. 5 shows the BEM model of computation.

Figs. 6 and 7 show the computed displacements u_x and stress σ_{xx} along the radial direction over the middle straight line, respectively. Figs. 8 and 9 show the computed displacements u_y and stress σ_{yy} along the ring direction interface over the middle curve line, respectively and Figs. 10 and 11 show the computed displacements u_x and stress σ_{xx} of the inner nodes, respectively. For comparison, results obtained using MDBEM [4] with the same node pattern are also provided. From Figs. 6–11, it can be seen that the presented IIBEM results are in very good agreement with MDBEM results, except for the two end nodes of Fig. 7 where the stress concentration effect may cause the discrepancy.

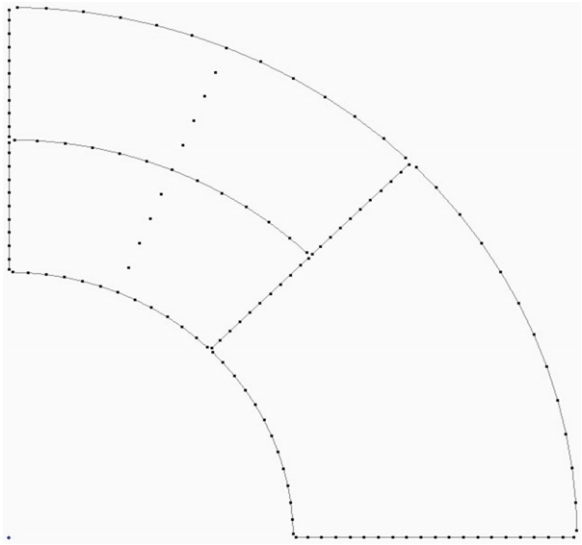

Fig. 5. BEM model of the three media cylinder.

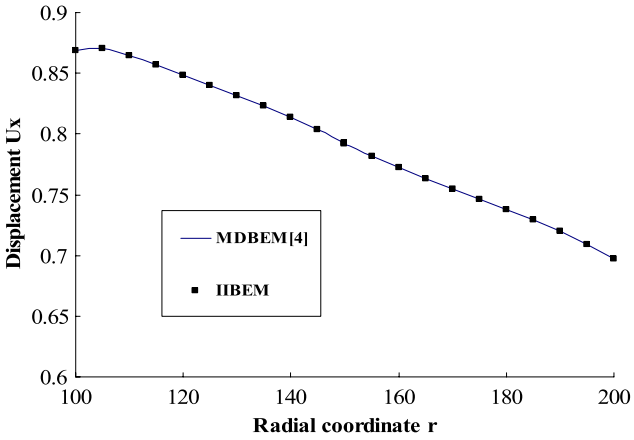

Fig. 6. Distribution of displacement u_x along radial direction.

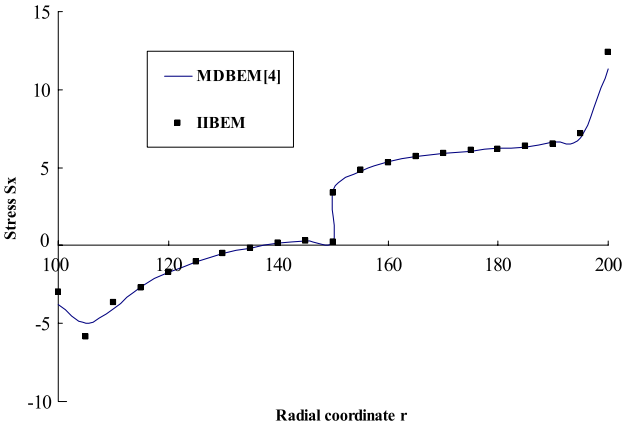

Fig. 7. Distribution of stress σ_{xx} along radial direction.

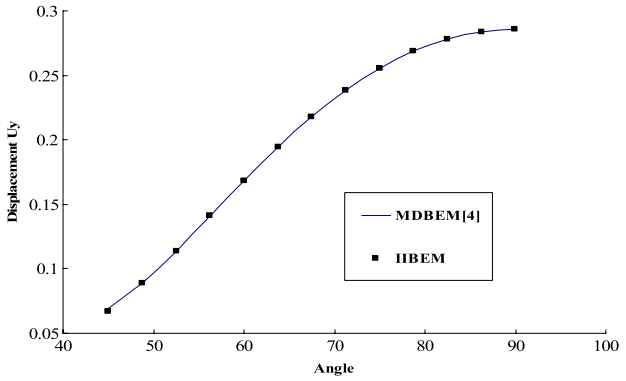

Fig. 8. Displacement in y direction over the middle curve line.

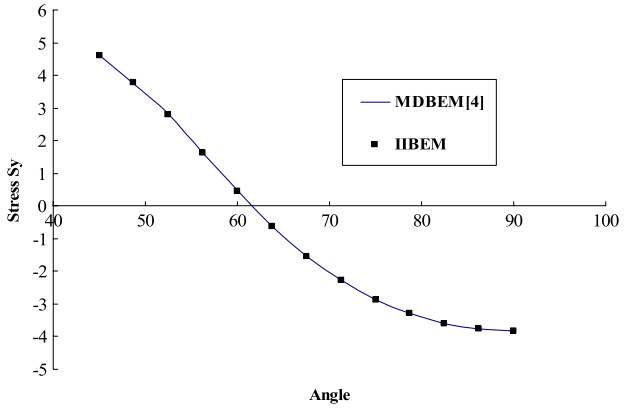

Fig. 9. Stress σ_{yy} over the middle curve line.

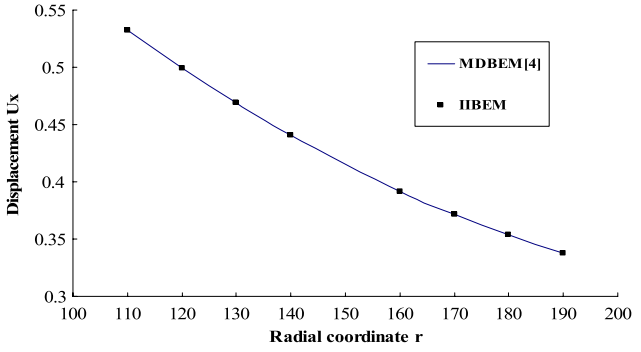

Fig. 10. Displacement in x direction at inner nodes.

Example 2 (*Plate with a Cylinder Consisting of Two Media Under Tensile Loading*)**.** A 3D rectangular plate with a cylinder, consisting of two media, with an internal diameter of 1.8 units and an external diameter of 2.7 units, is subjected to a uniform tensile loading of ten units ($P = 10$) as depicted in Fig. 12.

Due to symmetry, a quarter of the plate is analyzed. The geometry and boundary conditions of this example are shown in Figs. 12 and 13. The material properties are: shear modules of elasticity $\mu_1 = 4000$, $\mu_2 = 400$ and Poisson's ratio $\nu = 0.25$. Both the inner and outer circumferential lines are discretized into 20 equally-spaced quadratic boundary elements. The whole BEM model has a total of 254 outer boundary elements and 20 interface elements and 897 nodes. Fig. 14 shows the BEM model of computation.

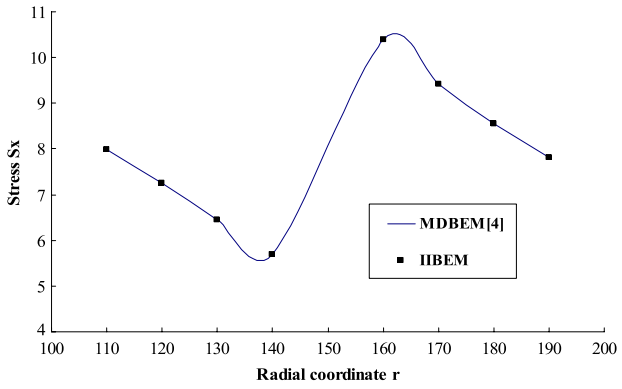

Fig. 11. Stress σ_{xx} at inner nodes.

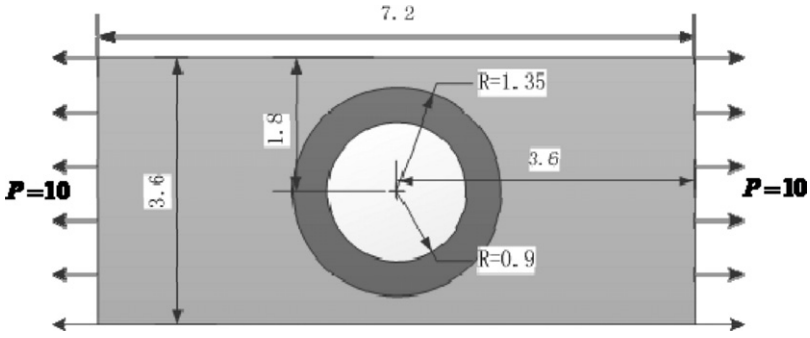

Fig. 12. Rectangular plate under tensile loading.

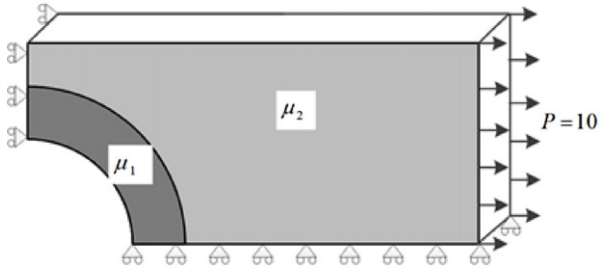

Fig. 13. A quarter of plate consisting of two media.

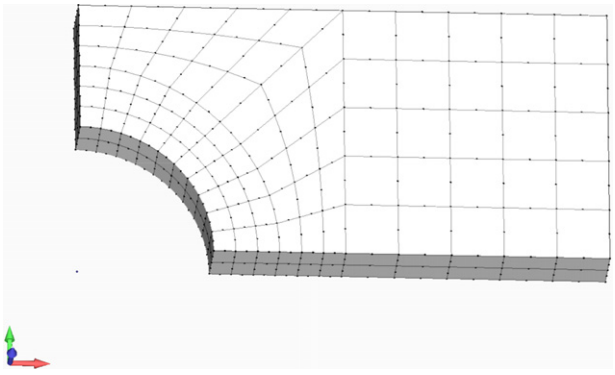

Fig. 14. BEM model of the two media plate.

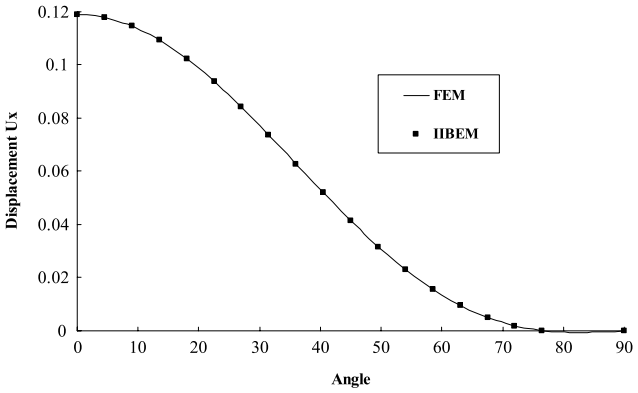

Fig. 15. Displacement in x direction over the interface curve line.

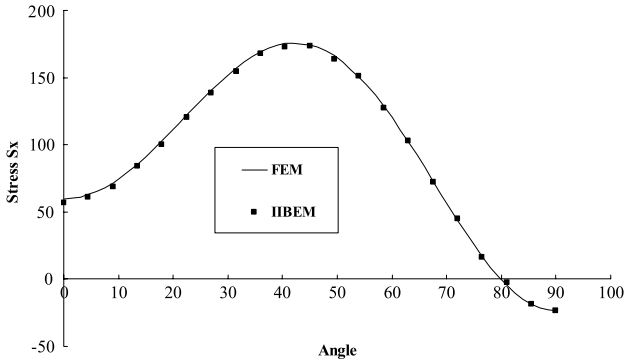

Fig. 16. Stress σ_{xx} over the interface curve line.

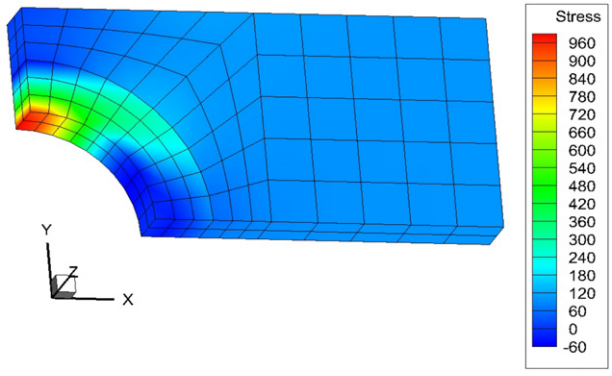

Fig. 17. Contour of the computed stress.

Figs. 15 and 16 show the computed displacements u_x and stress σ_{xx} along the ring direction interface over the middle curve line, respectively. For comparison, results obtained using FEM software ANSYS with the same node pattern are also provided. Fig. 17 shows the contour plot of the computed σ_{xx} stress.

From Figs. 15 and 16, it can be seen that the presented IIBEM results are in very good agreement with FEM results, although coarse meshes are used in BEM. In addition to be sure, the displacements computed using FEM are similar to those using the current IIBEM with the same coarse meshes as in IIBEM, but the accuracy of stresses using FEM is worse than using IIBEM. Therefore, to achieve a same accurate stress result, a finer mesh is necessary for FEM. This demonstrates the advantage of IIBEM over FEM in the meshing aspect.

6. Concluding discussions

In this paper, a new boundary element method (BEM) is developed for computing 2D and 3D multi-medium interface stresses. The main feature of the method is that a single integral equation is used to solve multiple-medium problems. Comparing to the commonly used conventional multi-domain boundary element method, it has the advantages of less labor effort in preparing the input data, fast evaluation of interface integrals, and no need to assemble the system of equations from individual medium's contributions.

By using the lately proposed method treating hyper-singular boundary integrals, the hyper-singular integrals appearing in the stress boundary integral equations can be evaluated precisely. Numerical examples have demonstrated the correctness of the developed method.

Acknowledgment

The authors gratefully acknowledge the National Natural Science Foundation of China for financial support to this work under Grant NSFC No. 11172055, 11202045.

References

[1] J.H. Kane, B.L. Kashava Kumar, S. Saigal, An arbitrary condensing noncondensing solution strategy for large scale, multi-zone boundary element analysis, Comput. Methods Appl. Mech. Engrg. 79 (1990) 219–244.
[2] C.Y. Dong, C.J. Pater, A boundary-domain integral equation for a coated plane problem, Mech. Res. Comm. 27 (2000) 643–652.
[3] X.W. Gao, T.G. Davies, 3D multi-region BEM with corners and edges, Int. J. Solids Struct. 37 (2000) 1549–1560.
[4] X.W. Gao, Three-step multi-domain BEM solver for nonhomogeneous material problems, Eng. Anal. Bound. Elem. 31 (2007) 965–973.
[5] C.B. Wang, J. Chatterjee, P.K. Banerjee, An efficient implementation of BEM for two- and three-dimensional multi-region elastoplastic analyses, Comput. Methods Appl. Mech. Engrg. 196 (2007) 829–842.
[6] G.I. Giannopoulos, N.K. Anifantis, A BEM analysis for thermomechanical closure of interfacial cracks incorporating friction and thermal resistance, Comput. Methods Appl. Mech. Engrg. 196 (2007) 1018–1029.
[7] X.W. Gao, J. Wang, Interface integral BEM for solving multi-medium heat conduction problems, Eng. Anal. Bound. Elem. 33 (2009) 539–546.
[8] X.W. Gao, K. Yang, Interface integral BEM for solving multi-medium elasticity problems, Comput. Methods Appl. Mech. Engrg. 198 (2009) 1429–1436.
[9] X.W. Gao, Source point isolation boundary element method for solving general anisotropic potential and elastic problems with varying material properties, Eng. Anal. Bound. Elem. 34 (2010) 1049–1057.
[10] X.W. Gao, W.Z. Feng, K. Yang, M. Cui, Projection plane method for evaluation of arbitrary high order singular boundary integrals, Eng. Anal. Bound. Elem. 50 (2015) 265–274.
[11] X.W. Gao, T.G. Davies, Boundary Element Programming in Mechanics, Cambridge University Press, 2002.
[12] X.W. Gao, The radial integration method for evaluation of domain integrals with boundary-only discretization, Eng. Anal. Bound. Elem. 26 (2002) 905–916.
[13] Ch. Zhang, M. Cui, J. Wang, et al., 3D crack analysis in functionally graded material, Eng. Fract. Mech. 26 (2002) 119–132.
[14] J.T. Chen, H.K. Hong, Review of dual boundary element methods with emphasis on hyper-singular integrals and divergent series, Appl. Mech. Rev. 52 (1999) 17–33.
[15] J. Sladek, V. Sladek, S.N. Atluri, Local boundary integral equation (LBIE) method for solving problems of elasticity with nonhomogeneous material properties, Comput. Mech. 24 (2000) 456–462.
[16] G.Z. Xie, F.L. Zhou, J.M. Zhang, X.S. Zheng, C. Huang, New variable transformations for evaluating nearly singular integrals in 3D boundary element method, Eng. Anal. Bound. Elem. 37 (2013) 1169–1178.
[17] G.I. Giannopoulos, N.K. Anifantis, Interfacial steady-state and transient thermal fracture of dissimilar media using the boundary element contact analysis, Internat. J. Numer. Methods Engrg. 62 (2005) 1399–1420.
[18] J.C. Lachat, J.O. Watson, Effective numerical treatment of boundary integral equation, Internat. J. Numer. Methods Engrg. 10 (1976) 991–1005.
[19] X.W. Gao, Ch. Zhang, J. Sladek, V. Sladek, Fracture analysis of functionally graded materials by a BEM, Compos. Sci. Technol. 68 (2008) 1209–1215.
[20] H.F. Peng, K. Yang, X.W. Gao, Element nodal computation-based radial integration BEM for non-homogeneous problems, Acta Mech. Sin. 29 (2013) 429–436.
[21] K. Yang, Y.F. Liu, X.W. Gao, Analytical expressions for evaluation of radial integrals in stress computation of functionally graded material problems using RIBEM, Eng. Anal. Bound. Elem. 44 (2014) 98–103.
[22] K. Yang, X.W. Gao, Y.F. Liu, Using analytical expressions in radial integration BEM for variable coefficient heat conduction problems, Eng. Anal. Bound. Elem. 35 (2011) 1085–1089.
[23] K. Yang, X.W. Gao, Radial integration BEM for transient heat conduction problems, Eng. Anal. Bound. Elem. 34 (2010) 557–563.
[24] X.W. Gao, K. Yang, Thermal stress analysis of functionally graded material structures using boundary element method, Chin. J. Theor. Appl. Mech. 43 (2011) 136–143.
[25] X.W. Gao, K. Yang, J. Wang, An adaptive element subdivision technique for evaluation of various 2D singular boundary integrals, Eng. Anal. Bound. Elem. 32 (2008) 692–696.